

Convection and Turbulence Effects in Strongly Driven Electrochemical Deposition

Carol Livermore* and Po-zen Wong†

Department of Physics and Astronomy, University of Massachusetts, Amherst, Massachusetts 01003
(Received 8 November 1993)

We study fast electrodeposition of zinc in a narrow channel using high magnification video microscopy to visualize the activities near the growth tips. We find that streamline and turbulent convection occur for different growth morphologies. In the regime of dendritic growth, we observed space charge fluctuations and the eruption of plumes. We probe the dynamics of such convective dendritic growth by applying an ac voltage on top of the dc deposition voltage. The ac current response shows a broad-band nonlinear behavior, in sharp contrast to the narrow-band linear behavior of diffusion-limited dendritic growth.

PACS numbers: 68.70.+w, 47.27.-i, 47.54.+r, 81.15.Pq

The morphology of electrochemically deposited metallic clusters has attracted much interest in recent years. The initial work of Brady and Ball on copper deposits [1] and that by Matsushita on zinc leaves [2] showed that fractal structures similar to diffusion-limited aggregates (DLA) could be grown by passing a dc current in an electrolytic cell. Many subsequent studies [3] found that other patterns could be formed by varying the applied voltage V and the electrolyte concentration C . Besides DLA-like fractals, dendritic needles and dense-random branching (DRB) morphologies were commonly observed. The latter was often called the dense-radial morphology because many experiments were done in a circular cell that resulted in a round outer envelope. However, the precise conditions for forming the different patterns were quite unpredictable and varied among different studies. This may be attributed to electrolyte convection, or the fact that nonlinear systems are inherently sensitive to delicate changes in the initial growth conditions, the boundary conditions, and the unknown surface condition of the electrodes. To better understand this problem, Kahanda *et al.* [4] recently studied the growth in the very slow tip velocity limit ($v_{\text{tip}} < 0.1 \mu\text{m}/\text{sec}$). They found that the treelike DLA pattern coarsened into a columnar structure due to local growth mechanisms. In this paper, we report a complementary study in the fast growth limit ($v_{\text{tip}} > 1 \mu\text{m}/\text{sec}$) where the DRB and dendritic morphologies occur.

The occurrence of the different patterns in fast electrodeposition presented a puzzle. If one assumes that the electrolyte is uniform and neutral everywhere (except in the *double layer* at the electrode surface that is less than 1 nm thick), then the static potential Φ obeys $\nabla^2\Phi = 0$. It is well known that such Laplacian growth would lead to either DLA-like fractals or dendritic needles depending on the crystalline anisotropy of the surface [5]. The DRB morphology cannot be explained. Allowing for concentration gradients and diffusion currents, the classical Nernst theory [5] showed that the assumption of charge neutrality and ion-number conservation in the *quasistatic limit* lead to $\nabla^2\mu^\pm = 0$ for the chemical potentials μ^+ and μ^- of the cations and anions, respectively. Here, μ^\pm are related

to the charge (q^\pm) and concentration (C^\pm) by $\mu^\pm = q^\pm\Phi + k_B T \ln C^\pm$. If the anion does not deposit, $\nabla^2\mu^- = 0$ implies that the anion migration and diffusion currents exactly cancel each other and the anion density is stationary. In that case, the only growth instability occurs at the cathode due to $\nabla^2\mu^+ = 0$ and the problem is unchanged.

To understand the cause of different morphologies, increasing attention is paid to the effect of electrolyte convection. Bruinsma and Alexander [6] noted that most experiments were performed at current densities far exceeding the diffusion limit of the Nernst theory, so that convection must be taken into account. In the presence of a flow field, spontaneous charge fluctuations are enhanced by the velocity gradients, which in turn generate gradients in the electrical force acting on the fluid body (electroconvection). This positive feedback mechanism results in an instability as the applied electric field is increased. There was, in fact, indirect evidence for such effects in an experiment by Suter and Wong [7]. They found that the current (or voltage) across the cell exhibited spontaneous oscillations in the regime of dendritic growth where the current density was high. This suggests the buildup and breakdown of space charge at the growth tips. Since then, Barkey and co-workers [8] and Fleury, Rosso, and Chazalviel [9] have observed electrolyte concentration gradients and fluid motion near the deposit at the cathode. In this paper, we present direct evidence for laminar and turbulent convection near the deposit and show how they are related to the growth morphology and the space charge fluctuations. We also show that the dynamics of dendritic growth in turbulent convection is like a *wide-band nonlinear amplifier*, in sharp contrast to the narrow-band linear behavior of dendrites grown by diffusion [10, 11].

The system we chose to study was the electrodeposition of zinc from ZnSO_4 solutions, in part because this is one of the most extensively studied systems [2, 3], but mainly because the current (or voltage) oscillations in Ref. [7] showed that there were space charge and nonlinear effects. Our aim was to use a high magnification microscope to observe the activities near the growth tips and relate them to the electrical signal. To visualize growth tips in a small

field of view with a shallow depth of field, we confined the growth in a channel that is both narrow and thin. It was formed by placing two parallel Teflon strips (0.13 mm thick) 1 mm apart and clamped between two 1/4 in. thick acrylic plates. Holes were drilled through the top plate to insert 1 mm diam zinc wires as electrodes and to inject ZnSO_4 solutions into the channel. The distance between the working (cathode) and counter (anode) electrodes varied between 5 and 21 mm as needed. Additional electrodes were placed at other points to make four-terminal ac resistance measurements, and to monitor the voltage drop in different sections of the channel. These electrodes were offset from the channel by 3 mm so that they are not in the current path.

The cell was placed over a 2 in. hole on a platform, with a fiber optic lamp illuminating from above. All the electrical connections were made above the cell. A small monochrome video microscope was placed under the platform in an inverted position to view the growth from below through the hole. It was mounted on an XYZ translator for focusing and moving along the channel to follow the growth. The field of view was $1.6 \times 1.2 \text{ mm}^2$ and it could be digitized to 640×480 square pixels ($2.5 \mu\text{m}/\text{pixel}$) on a computer. High contrast features above 2 pixels could be resolved. The solution concentration we used was between 0.03M and 1.0M with typical cell resistance in the range of 5–200 k Ω . We applied constant voltages between 5 and 30 V across the cell to generate currents up to a few mA. The average current density in the channel exceeded $1 \text{ A}/\text{cm}^2$ in the most rapid growths. Oscillation amplitudes larger than 1% were common (e.g., see Fig. 2). Time series of the current were recorded by an HP-35665A dynamic signal analyzer which monitored the voltage across a series resistor (100 or 200 Ω). Tip velocity was in the approximate range of 1–100 $\mu\text{m}/\text{sec}$, comparable to those reported in Ref. [7].

Figure 1 illustrates the range of morphology we observed. It varied mainly with the electrolyte concentration (C), and much less with the applied voltage (V) or current (I). The deposits had DRB morphology for $C \leq 0.1M$, but they were mostly dendritic for $C \geq 0.3M$. Between these two regimes, a mixed morphology occurred. Figure 1(a) shows an example of the DRB pattern grown in 0.1M solution, and Fig. 1(c) is a well-formed dendrite grown in 0.5M solution. The cell currents in the two cases were almost identical (0.66 and 0.68 mA, respectively) but the tip velocities (v_{tip}) were very different: about 100 $\mu\text{m}/\text{sec}$ for the DRB and 15 $\mu\text{m}/\text{sec}$ for the dendrite. Figure 1(b) illustrates a case of mixed morphology deposits grown with $C = 0.3M$, $I = 0.80 \text{ mA}$, and $v_{\text{tip}} \approx 75 \mu\text{m}/\text{sec}$. It is noteworthy that, for about the same current, (v_{tip}) is higher for lower concentrations. In each case, (v_{tip}) is approximately the same as the calculated drift velocity (v_d) of the ions. This implies that the growth is migration limited. More examples of growth morphology are given in Ref. [12]. Here, we focus on the effects of fluid convection and space charge fluctuations.

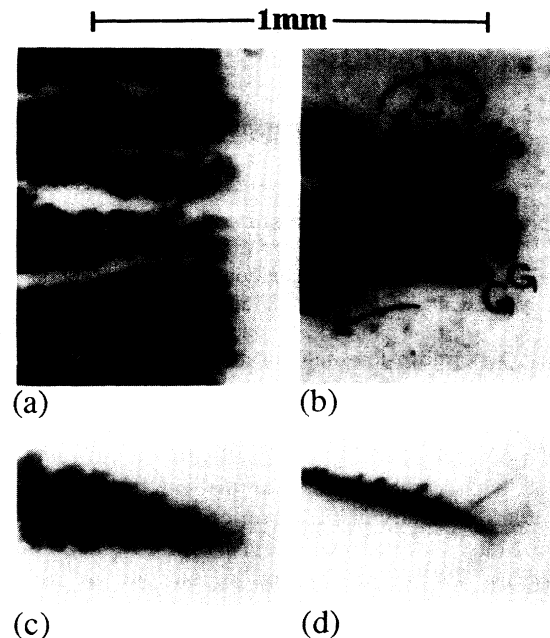


FIG. 1. Examples of DRB morphology in (a), mixed morphology in (b), and dendritic growth in (c) and (d). Tracer particles in (b) show the fluid convection patterns. Shadows in (c) and (d) show concentration variations. See text for growth conditions.

The direct observation of fluid convection was made possible by suspending chemically inert polymer spheres (Duke Scientific No. 5200, $2.0 \mu\text{m}$ diameter) in the electrolyte as tracer particles. They formed small aggregates that were readily visible. The small negative charge on the spheres made them drift slowly towards the anode in the bulk electrolyte. Near the deposit, however, a variety of fluid motion was observed and is indicated in Fig. 1(b). Close to the growth front, the particles were drawn to the cathode despite their negative charge, indicating the viscous drag from the cation migration. As the depleted fluid must move out for cation-rich fluid to move in, swirling occurred near the tips. The arrows in Fig. 1(b) depict the flow patterns seen in our continuous video recording. Besides the strong actions near the tips, some particles slid down the outside of the deposit and some particles in the fjords migrated outward. This shows that some of the momentum of the depleted fluid carries it into the interior of the deposit and pushes the anion-rich fluid out of the deposit. These streamlines create viscous forces and Bernoulli pressure that stretched and squashed the DLA-like pattern into the compact DRB pattern as the flow velocity increased. Bending and stretching of the branches were most visible in dilute solutions where the DRB pattern is formed. The smooth outer envelope of the DRB pattern in Fig. 1(a) can be attributed to the depletion front of the anion density field. It does not have Mullins-Sekerka-type instabilities because a high resistivity region is left behind the front. That the anion-rich fluid is pushed out by the depleted fluid may also contribute to the stabil-

ity of this envelope. Similar effects have been seen in fluid mixing [8].

To investigate the ion concentration fluctuations near the tips, we used a qualitative Schlieren method [13]. We positioned the light beam at a slight angle from the optical axis of the microscope such that the edge of the beam just caught the objective lens. Concentration variation in the electrolyte led to spatial inhomogeneity in the refractive index ($dn/dC \approx 0.02/M$ in $ZnSO_4$) that bent some light rays away from the lens and some towards it, resulting in brightness variation in the image field. Interference effects due to multiple reflections between the top and bottom plates of the cell probably also contributed to the intensity pattern. Figure 1(c) is an example in which we can see the shadowing effects near the tip. The contrast from these shadows can be enhanced by using linearly polarized incident light. Figure 1(d) shows such an example obtained with $C = 0.5M$, $I = 1.33$ mA, and $v_{tip} \approx 150$ $\mu\text{m}/\text{sec}$. While we did not attempt to quantify the intensity variation, we do know that it came from concentration inhomogeneity because the shadows faded away when the growth was stopped. Most interestingly, in real-time video recordings of dendritic growth, we were sometimes able to see remarkable pulsations of these shadows. For example, the shadows in Fig. 1(c) pulsed at about 0.7 Hz, which was the same frequency as the current oscillation at the same instant. Because v_{tip} was also slow in this case, we were able to see *clearly* that the pulsations came from little *plumes* emitted at the tips of the dendrite at fairly regular intervals, much like those seen in turbulent Rayleigh-Bénard convection [14]. These plumes are indicative of the breakdown of a thin boundary layer in which the laminar flow diminishes. Not all shadows could be seen to oscillate, however. The video speed of 30 frames/sec and the small image field limited us to cases where both the frequency and v_{tip} were low. For example, the case in Fig. 1(d) had oscillations near 1 Hz, but the tip passed through the image field in a few seconds. Only brief flickering could be recorded.

To investigate space charge fluctuations associated with the current and concentration oscillations, two reference electrodes are placed a few millimeters in front of the cathode and anode (offset from the current path) to measure the voltage drop in the three sections of the channel: cathode, bulk electrolyte, and anode. Charge accumulation at the interface is marked by a change in voltage (δV) that is opposite to the change in cell current (δI). The voltage drop in the cathode section (V_c) consists of the cathode interfacial voltage and some IR drop in the electrolyte. The voltage drop in the bulk between the two reference electrodes (V_e) is mainly an IR drop, and the voltage drop in the anode section (V_a) reveals the anode interfacial voltage. Our results show that V_c always oscillates out of phase with the cell current I , while V_e and V_a are always in phase with I . Figure 2 depicts this behavior for the case of $C = 0.5M$, $I = 0.23$ mA, and $v_{tip} = 5$ $\mu\text{m}/\text{sec}$. Here, δV is normalized by the mean voltage (V) across each sec-

tion and compared to the normalized cell current variation $\delta I/I$. The top two time series show V_c oscillates out of phase with I . The lower four traces show that both V_e and V_a oscillate in phase with I . This proves that space charge fluctuations occur near the cathode deposit. Although this result does not tell us the size of the space charge region, given that the current oscillation frequency matches the shadow pulsing in Fig. 1(c) and the mechanism of electroconvection requires the space charge to be extended, it is safe to conclude that space charge exists in the entire region where shadow and fluid motion are observed. This implies that the usual diffusion-limited (Laplacian) growth model is inapplicable because cation transport is limited by fluid convection and Poisson's equation must be used in place of Laplace's equation. There is presently no theoretical understanding of such *convection-limited growth* phenomena.

To provide some quantitative information on *convection-limited growth*, we studied how the current oscillations in the dendritic regime respond to an applied voltage. We note that in studies of directional solidification and Saffman-Taylor fluid flow problems, both theories [10] and experiments [11] have shown that the tips behave like *narrow-band linear amplifiers* driven by random noise and emit incoherent side branches with fairly well defined wavelengths. When perturbed by a coherent ac signal at a fixed frequency, the side branches became very well ordered. In our experiment, we perturbed the dendritic growth by applying an ac voltage with an amplitude equal to 10% of the dc deposition voltage ($\delta V/V_{dc} = 10\%$). The response of the dendrite is manifested by the normalized ac current ($\delta I/I_{dc}$). We found that in most cases, the ac/dc ratio was increased

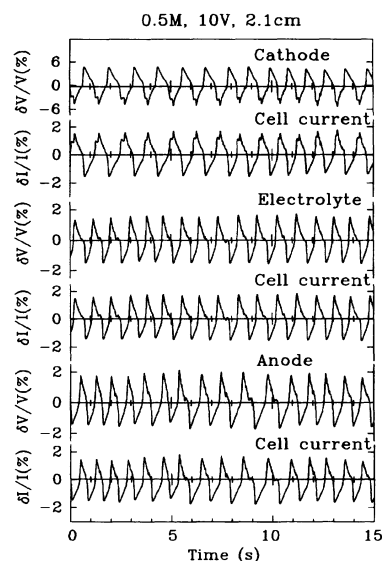


FIG. 2. The voltage oscillations across the cathode interface (V_c), the bulk electrolyte (V_e), and the anode interface (V_a) are each compared to the cell current (I) oscillations. The first pair of traces show V_c out of phase with I . The two lower pairs of traces show V_e and V_a in phase with I (see text).

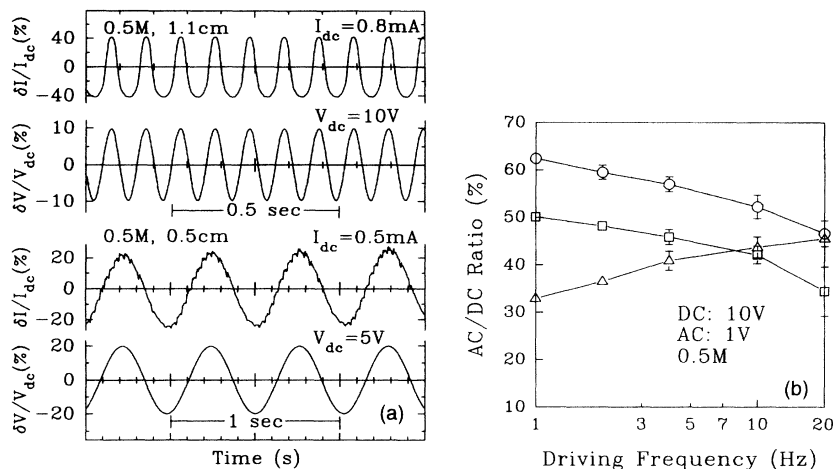


FIG. 3. (a) A 10% variation in the applied voltage results in 40% nonlinear current oscillations during convective dendritic growth (top two traces). In rare occasions, however, no amplification could be detected (bottom two traces). (b) Sweeping the frequency of the applied voltage up (\circ and \square) and down (\triangle) during dendritic growth showed a fairly broad frequency response in $\delta I/I_{dc}$. The variation is almost entirely due to the increase in I_{dc} as the channel is shortened during the sweep.

several-fold over a wide frequency range and the behavior is highly nonlinear. The top two traces in Fig. 3(a) illustrate a case with a sinusoidal δV at 10 Hz. The resulting current wave form is clearly distorted and $\delta I/I_{dc} \approx 40\%$, i.e., the ac gain is 4. Figure 3(b) shows the $\delta I/I_{dc}$ response from 1 to 20 Hz measured in three separate runs under the same conditions with the applied voltage frequency sweeping up (\circ and \square) and down (\triangle). In each case, the ac/dc ratio changed by less than 30% during the sweep. This change was actually almost entirely due to the increase in I_{dc} during the sweep as the channel length became shorter. δI was essentially constant in each case. Thus the dynamical response of the convectively grown dendrites is more like a *wide-band nonlinear amplifier*. This behavior is intuitively reasonable because the turbulent environment has a wide spectral content. It is also interesting to note that the gain of this amplifier is unpredictable from run to run, which is evident in Fig. 3(b). There are some occasions where the dendrite did not lock onto the applied ac voltage. The two lower traces in Fig. 3(a) show a case with $\delta I/I_{dc} = \delta V/V_{dc}$ for a 2 Hz applied voltage. A small spontaneous current oscillation at 35 Hz can be seen as the small ripples in $\delta I/I_{dc}$.

In summary, we have presented evidence that the morphological changes in fast electrochemical deposition are related to the increasing importance of convective transport as v_{tip} exceeds $1 \mu\text{m}/\text{sec}$. Viscous forces and Bernoulli pressure from streamline flow distort the DLA-like pattern into the more compact DRB pattern. Dendrite formation is associated with turbulent convection with violent space charge fluctuations and plume emissions. The dynamics of such convective dendritic growth is distinctly different from diffusive growth.

This work is supported by the National Science Foundation under Grant No. DMR-8922830, with supplemental grants from the Research Experience for Undergraduates program.

*Present address: Department of Physics, Harvard University, Cambridge, MA 02138.

[†]Electronic address: PZWONG@PHAST.UMASS.EDU

- [1] R. M. Brady and R. C. Ball, *Nature (London)* **309**, 225 (1984).
- [2] M. Matsushita, M. Sano, Y. Hayakawa, H. Honjo, and Y. Sawada, *Phys. Rev. Lett.* **53**, 286 (1984); M. Matsushita, Y. Hayakawa, and Y. Sawada, *Phys. Rev. A* **32**, 3814 (1985).
- [3] See, e.g., Y. Sawada, A. Dougherty, and J.P. Gollub, *Phys. Rev. Lett.* **56**, 1260 (1986); D. Grier, E. Ben-Jacob, Roy Clarke, and L. M. Sander, *Phys. Rev. Lett.* **56**, 1264 (1986); **59**, 2315 (1987); G. L. M. K. S. Kahanda and M. Tomkiewicz, *J. Electrochem. Soc.* **136**, 1497 (1989).
- [4] G. L. M. K. S. Kahanda, X.-q. Zou, R. Farrell, and P.-z. Wong, *Phys. Rev. Lett.* **68**, 3741 (1992); **71**, 806 (1993).
- [5] See, e.g., L. M. Sander, in *The Physics of Structural Formation*, edited by W. Guttinger and G. Dangelmayr (Springer-Verlag, Berlin, 1987) p. 257; V. G. Levich, in *Physicochemical Hydrodynamics* (Prentice-Hall, London, 1962).
- [6] R. Bruinsma and S. Alexander, *J. Chem. Phys.* **92**, 3074 (1990).
- [7] R. M. Suter and P.-z. Wong, *Phys. Rev. B* **39**, 4536 (1989).
- [8] D. P. Barkey, *J. Electrochem. Soc.* **138**, 2912 (1991); D. P. Barkey and D. P. LaPorte, *ibid.* **137**, 1655 (1990); P. Garik, J. Hetrick, B. Orr, D. Barkey, and E. Ben-Jacob, *Phys. Rev. Lett.* **66**, 1606 (1991).
- [9] V. Fleury, M. Rosso, and J.-N. Chazalviel, *Phys. Rev. Lett.* **68**, 2492 (1992); *Phys. Rev. E* **48**, 1279 (1993).
- [10] R. Pieters and J. S. Langer, *Phys. Rev. Lett.* **56**, 1948 (1986); D. A. Kessler and H. Levine, *Europhys. Lett.* **4**, 215 (1987).
- [11] M. Rabaud, Y. Couder, and N. Gerard, *Phys. Rev. A* **37**, 935 (1988); Ph. Bouissou, A. Chiffaudel, B. Perrin, and P. Tabling, *Europhys. Lett.* **13**, 89 (1990); L. M. Williams, M. Muschol, X. Qian, W. Losert, and H. Z. Cummins, *Phys. Rev. E* **48**, 489 (1993).
- [12] C. Livermore, Honors thesis, University of Massachusetts, 1993.
- [13] See, e.g., L. A. Vasil'ev, in *Schlieren Methods*, translated by A. Baruch (Israel Prog. for Sci. Translation, New York, 1971).
- [14] See, e.g., T. H. Solomon and J. P. Gollub, *Phys. Rev. Lett.* **64**, 2382 (1990), and references therein.

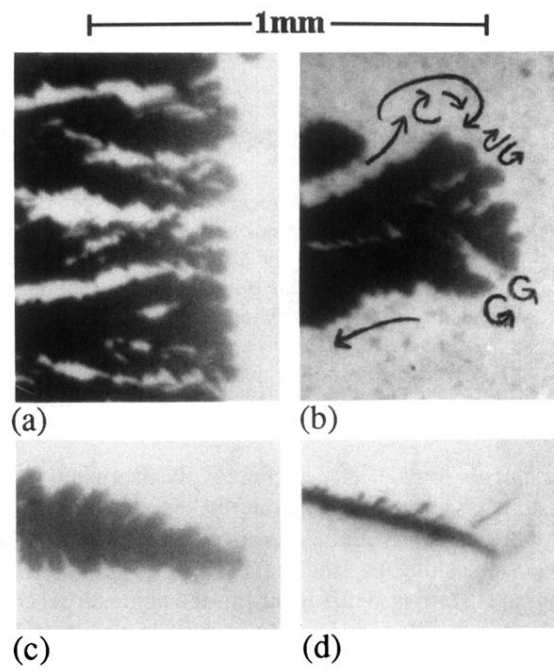


FIG. 1. Examples of DRB morphology in (a), mixed morphology in (b), and dendritic growth in (c) and (d). Tracer particles in (b) show the fluid convection patterns. Shadows in (c) and (d) show concentration variations. See text for growth conditions.